BIOCHEMISTRY
including biophysical chemistry & molecular biology

Article

pubs.acs.org/biochemistry

Crystal Structures and Functional Characterization of Wild-Type CYP101D1 and Its Active Site Mutants

Dipanwita Batabyal and Thomas L. Poulos*

Departments of Molecular Biology and Biochemistry, Chemistry, and Pharmaceutical Sciences, University of California, Irvine, California 92697-3900, United States

ABSTRACT: Although CYP101D1 and P450cam catalyze the same reaction at similar rates and share strikingly similar active site architectures, there are significant functional differences. CYP101D1 thus provides an opportunity to probe what structural and functional features must be shared and what features can differ but maintain the high catalytic efficiency. Crystal structures of the cyanide complex of wild-type CYP101D1 and it active site mutants, D259N and T260A, have been determined. The conformational changes in CYP101D1 upon cyanide binding are very similar to those of P450cam, indicating a similar mechanism for proton delivery during oxygen activation using solvent-assisted proton transfer. The D259N−CN^- complex shows a perturbed solvent structure compared to that of the wild type, which is similar to what was observed in the oxy complex of the corresonding D251N mutant in P450cam. As in P450cam, the T260A mutant is highly uncoupled while the D259N mutant gives barely detectable activity. Despite these similarities, CYP101D1 is able to use the P450cam redox partners while P450cam cannot use the CYP101D1 redox partners. Thus, the strict requirement of P450cam for its own redox partner is relaxed in CYP101D1. Differences in the local environment of the essential Asp (Asp259 in CYP101D1) provide a strucutral basis for understanding these functional differences.

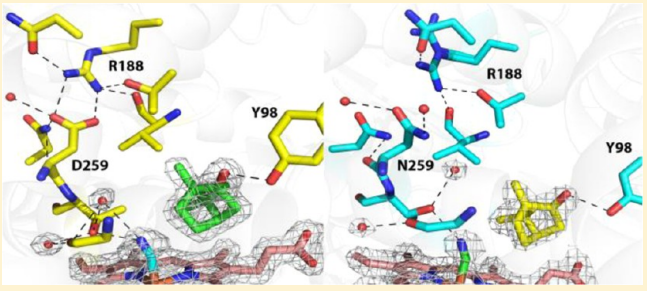

Cytochromes P450 catalyze a variety of monooxygenase reactions that require the transfer of an electron from redox partners. P450cam, a soluble bacterial cytochrome from *Pseudomonas putida* that hydroxylates camphor, has served as the primary model for addressing questions about the detailed mechanisms of electron transfer and O_2 activation. The entire P450cam system consists of an iron−sulfur ferredoxin, putdiaredoxin (Pdx), that transfers electrons from the flavin adenine dinucleotide protein, putidaredoxin reductase (Pdr), to P450cam. P450cam is unusual in having a strict and specific requirement for Pdx as an electron donor, which suggests that the specificity for Pdx is related to the Pdx-induced structural change required for oxygen activation.[1−3] The recent P450cam−Pdx crystal and nuclear magnetic resonance structures[4,5] indicate that the effector role of Pdx is to shift P450cam toward the open conformation, which allows the establishment of a water-mediated H-bonded network that is required for proton-coupled electron transfer and oxygen activation.[5] Pdx binding has been proposed to free the critical residue, Asp251, from salt bridging interactions with Arg186 and Lys178 so that it can serve its catalytic function[6,7] in shuttling protons to dioxygen.

CYP101D1 is a close homologue of P450cam and catalyzes exactly the same camphor hydroxylation reaction, uses a similar ferredoxin (Arx) and ferredoxin reductase (Adr), but exhibits subtle and possibly important differences.[8] Adjacent to the heme iron ligand, Cys357, is Leu358 in P450cam, while this residue is Ala in CYP101D1. Leu358 plays a role in binding of the P450cam redox partner, putidaredoxin (Pdx).[9] On the opposite side of the heme approximately 15−20 Å away, the critical residue Asp251 in P450cam forms strong ion pairs with Arg186 and Lys178. In CYP101D1, a Gly replaces Lys178. Thus, the local electrostatic environment and ion pairing are substantially different in CYP101D1. Another important difference relates to the effect of K^+ ions on substrate binding and spin state. Potassium ions promote both substrate binding and high-spin P450cam.[10] P450cam has a K^+ binding site near Tyr96 whose side chain OH group forms hydrogen bonds with the camphor carbonyl oxygen of camphor, so K^+ helps to stabilize key substrate−protein interactions.[11] CYP101D1 lacks this K^+ binding site, and K^+ has an only modest effect on the fraction of high-spin CYP101D1.[8] The addition of 200 mM KCl to the CYP101D1−camphor complex increases the level of the spin state from 30% to only 40%.[8] In our recent study aimed at comparing these two enzymes, these sites were systematically mutated in P450cam to the corresponding residues in CYP101D1.[12] The data show that although individually the mutations have little effect on activity or structure, in combination there is a major decrease in enzyme activity because the mutants are locked in the low-spin state, thus preventing the transfer of electrons from the P450cam redox partner, Pdx. Overall, these results illustrate the delicate

Received: September 27, 2013
Revised: November 19, 2013
Published: November 21, 2013

balance between the open and closed conformational states[13] as well as a strong structural connection between the Pdx binding site (Leu358) and the region around Asp251 that undergoes a large structural change in the open−closed transition in P450cam. The results along with some structural and biochemical studies of CYP101D1 indicate that these complex interactions among spin state, redox partner binding, and conformational changes might be less stringent or different in CYP101D1 primarily because this P450 is a predominantly low-spin species even in the presence of substrate[14] but still is as active as P450cam. This opens up some interesting questions about how two such similar forms of P450 can behave so differently and what, if any, the connection is among these various levels of conformational dynamics, activity, and biological function. Here we present the crystal structures of cyanide- and camphor-bound complexes of wild-type CYP101D1 and its active site mutants, D259N and T260A, and enzyme activities. Because CYP101D1 is so similar to P450cam, a comparison of the two with respect to redox partner specificity has also been addressed to improve our understanding of whether the effector/allosteric role of redox partner binding is a general property of P450 proteins or is unique to P450cam.

EXPERIMENTAL PROCEDURES

Protein Expression and Purification. The *Escherichia coli* codon-optimized genes encoding full-length ArR, Arx, and CYP101D1 were subcloned into vector pET28a (Novagen Inc.). An N-terminal six-His tag was incorporated for both CYP101D1 and PdR. The Arx gene was subcloned without the six-His tag. All proteins were expressed in *E. coli* strain BL21(DE3).

For expression of wild-type and mutant CYP101D1, ArR, and Arx, cells were grown at 37 °C in 1 L flasks of Luria-Bertani broth (LB) medium containing the appropriate antibiotic until the optical density at 600 nm reached 0.6−0.8. Recombinant protein production was induced with 1 mM isopropyl 1-thio-D-galactopyranoside overnight at 25 °C, after which cells were harvested by centrifugation and resuspended in respective lysis buffers for further purification as described below.

For CYP101D1 (and its mutants), pink cell pellets were resuspended in 50 mM potassium phosphate (pH 7.4) and 150 mM NaCl and then lysed by sonication at 4 °C. The crude extracts were centrifuged at 16000 rpm for 1 h, and the supernatant was loaded onto a Ni-IMAC column (Bio-Rad). The column was washed with lysis buffer containing 10 mM imidazole, and the target protein was eluted with elution buffer [50 mM potassium phosphate (pH 7.4) and 300 mM imidazole]. The pooled fractions were concentrated and then buffer-exchanged into 50 mM potassium phosphate and incubated for 4−5 h with high-purity thrombin (bovine) at room temperature (approximately 10 units of thrombin/mg of CYP101D1) to cleave the His tag. The incubated mixture was reloaded into the Ni-IMAC column, and the flow through was collected and concentrated and buffer exchanged with 20 mM Tris (pH 8.0) and 1 mM DTT. The protein was further purified on a Hi Trap Q column (GE Healthcare) using a linear gradient from 0 to 1 M NaCl in 20 mM Tris (pH 8.0) and 1 mM DTT. Gel filtration chromatography on a Superdex 75 (GE Healthcare) column was used to obtain highly pure CYP101D1 using a buffer that consisted of 20 mM Tris (pH 8.0) and 1 mM DTT.

ArR was purified using the Ni-IMAC column as described for CYP101D1 using the same buffer composition. The eluate from the Ni column was concentrated and loaded on Superdex 75 as described in the protocol for CYP101D1.

For Arx purification, the brown cell pellet was resuspended in 50 mM potassium phosphate (pH 7.4) and 1 mM DTT. After sonication and high-speed centrifugation, the supernatant was loaded on DEAE-Sepharose fast flow (GE Healthcare). The column was washed, and the protein was eluted with a gradient from 50 to 500 mM NaCl in 50 mM potassium phosphate (pH 7.4) and 1 mM DTT. The fractions containing Arx were pooled together and further purified using Superdex 75 (GE Healthcare) using a buffer that consisted of 20 mM Tris (pH 8), 150 mM NaCl, and 1 mM DTT.

Pdr and Pdx were expressed and purified using previously established protocols.[15,16]

Spectroscopic Studies. All UV−visible spectroscopy was performed using a Cary 3 spectrophotometer. The CYP101D1 content was measured using an extinction coefficient of 107 mM^{-1} cm^{-1} at 418 nm.[17] Concentrations of Arx and ArR were calculated using extinction coefficients of 9.3 mM^{-1} cm^{-1} at 414 nm and 10.0 mM^{-1} cm^{-1} at 458 nm, respectively.[17] Concentrations of Pdx and Pdr were calculated using extinction coefficients of 5.9 mM^{-1} cm^{-1} at 455 nm and 11.0 mM^{-1} cm^{-1} at 454 nm, respectively.[18,19]

Enzyme Assays. Cytochrome P450 hydroxylation activity was determined in the complete system of three proteins (CYP101D1, ArR, and Arx) by measuring rates of camphor-dependent NADH oxidation at 25 °C following previously established protocols.[20] The concentration of proteins and substrates used ensured that the rates measured were under steady state saturating conditions. Briefly, the reaction mixture of 1.2 mL contained 0.5 μM ArR, 5 μM Arx, and 0.5 μM P450 in 50 mM Tris (pH 7.4). The rate of NADH oxidation was measured by monitoring the absorbance change at 340 nm using an extinction coefficient of 6.22 mM^{-1} cm^{-1}. The reaction was initiated by first adding NADH (final concentration of 200 μM) in the absence of camphor to obtain the background rate. Substrate-dependent NADH oxidation was then assayed in the presence of 200 μM camphor and was calculated as the difference between the measured rate and the rate of nonspecific NADH oxidation in the absence of camphor (background). The assay was repeated with a final camphor concentration of 1 mM. After the completion of the reaction (followed by UV−vis), the reaction mixture was subjected to organic extraction with dichloromethylene for product formation analysis using GC−MS according to the previously established protocol.[21]

Crystallization of Wild-Type CYP101D1 and Its Mutants. All protein (wild-type or mutant CYP101D1) crystals were grown at room temperature using the hanging drop vapor diffusion method in 100 mM Tris-HCl buffer (pH 8.2) and 1.4−1.6 M ammonium sulfate as the reservoir solution. The initial droplets contained 2 μL of protein solution at a concentration of ∼30−35 mg/mL, and 2 μL of the reservoir solution was equilibrated against 500 μL of the reservoir solution. To generate camphor-bound crystals, individual CYP101D1 crystals were soaked in reservoir solution containing saturated camphor and 20% glycerol (as a cryoprotectant) for 1−2 h and flash-cooled with liquid nitrogen. To generate the cyanide- and camphor-bound complex of CYP101D1 and its mutants, the same protocol for generating the camphor-bound complex was used and the

Table 1. Crystallographic Data Collection and Refinement Statistics[a]

	CYP101D1 bound to camphor	CYP101D1 bound to camphor and cyanide	substrate-free CYP101D1 bound to glycerol	D259N CYP101D1 bound to camphor	D259N CYP101D1 bound to camphor and cyanide	T260A CYP101D1 bound to camphor
PDB entry	4C9K	4C9L	4C9M	4C9N	49CO	4C9P
			Data Collection			
space group	$P6_422$	$P6_422$	$P6_422$	$P6_422$	$P6_422$	$P6_422$
resolution (Å)	2.18	1.81	1.80	2.30	1.98	1.80
radiation source	SSRL 7-1	SSRL 7-1	SSRL 7-1	SSRL 7-1	SSRL 7-1	SSRL 11-1
completeness (%)	99.2 (99.2)	99.7 (99.3)	99.9 (100)	100 (100)	100 (100)	99.8 (98.6)
no. of unique reflections	69832 (9954)	121806 (5915)	121820 (5966)	59543 (8519)	94411 (4631)	123065 (17526)
redundancy	14.2 (14.3)	9.4 (8.0)	10.6 (10.1)	20.5 (16.8)	22.7 (14.5)	16.2 (14.9)
R_{sym} or R_{merge}	0.085 (0.49)	0.076 (0.38)	0.075 (0.26)	0.211 (1.06)	0.169 (0.742)	0.084 (1.07)
R_{pim}	0.023 (0.133)	0.036 (0.126)	0.034 (0.126)	0.034 (0.126)	0.047 (0.260)	0.021 (0.28)
$I/\sigma(I)$	28.5 (7.0)	16.4 (4.4)	18.5 (6.2)	15.0 (4.2)	30.15 (3.8)	22.3 (3.0)
			Refinement			
resolution (Å)	2.18	1.80	1.80	2.20	1.97	1.79
B factor (mean) (Å^2)	30.81	23.67	23.20	35.65	23.16	30.02
R_{work}	0.175	0.152	0.154	0.176	0.157	0.168
R_{free}	0.218	0.182	0.188	0.208	0.185	0.193
root-mean-square deviation for bonds (Å)	0.007	0.011	0.01	0.008	0.010	0.007
root-mean-square deviation for angles (deg)	1.155	1.402	1.353	1.153	1.317	1.192
no. of atoms						
protein	6496	6496	6496	6504	6504	6476
ligand/ions	130	110	92	130	110	92
water	543	977	927	485	819	782

[a]Values for the highest-resolution shell are given in parentheses. Because R_{merge} tends to increase with high multiplicity, R_{pim}, which is a multiplicity-corrected version, is also reported here.[38]

reservoir solution in addition contained 50−60 mM KCN. For substrate-free conditions, crystals were soaked in a reservoir solution containing 20% glycerol for 15−20 min and then flash-frozen.

All data were collected remotely using the Stanford Synchrotron Radiation Lightsource (SSRL) beamline as indicated in Table 1. Data were indexed, integrated, and scaled with either MOSFLM,[22] XDS,[23] or HKL2000.[24] Molecular replacement calculations were conducted with Phaser[25] through the CCP4i[26] graphic interface using ferric camphor-bound wild-type CYP101D1 [Protein Data Bank (PDB) entry 3LXI] as a search model. Further structure refinements were performed using Phenix.refine.[27] Table 1 lists data collection and refinement statistics.

Calculation of Salt Bridge Stability. To compare the strength of salt bridges involving a conserved Asp-Arg pair (Asp251-Arg186 in P450cam and Asp259-Arg188 in CYP101D1), the procedures used by Lounnas and Wade[28] adapted from Hendsch and Tidor[29] and Delphi[30] were used. Each crystal structure was protonated and energy minimized using Amber,[31] and Delphi calculations were conducted using full Amber charges. The stability of the salt bridge is given as $\Delta G_{tot} = \Delta G_{sol} + \Delta G_{prt} + \Delta G_{brd}$, where ΔG_{sol} is the solvation energy, ΔG_{prt} is the energy of the interaction of the side chains with the protein, and ΔG_{brd} is the bridging interaction energy between side chains. For these calculations, charges were either turned off (set to zero) or left on. ΔG_{solv} is the sum of grid energies for the Asp in water, Arg in water, Asp with charges on in the protein with the rest of the protein charges off, and the same calculations with the Arg side chain. ΔG_{prt} is the sum of grid energies for all charges on, both side chain charges on and protein charges off, and both side chains with charges off and protein charges on. ΔG_{brd} is the sum of grid energies of the Asp with charges on and the protein charges off, the Arg with charges on and the protein charges off, and both side chain charges on and the protein charges off. The internal and external dielectric constants were set to 4.0 and 80.0, respectively, at a salt concentration of 0.1M. The grid size was 0.5 Å per grid, and only a single calculation was conducted.

RESULTS

Substrate-Free and -Bound Crystal Structures. These structures already have been determined,[8] and here we present two new observations. Although the active sites of CYP101D1 and P450cam are nearly identical, one notable difference is that there is extra density extending from C5 of camphor that we interpret as the product, 5-*exo*-hydroxycamphor (Figure 1A,B). This extra density could be due to a nonproductive binding mode of camphor with the carbonyl oxygen oriented toward the iron. This, however, is very unlikely because the extra desnity is clearly attached to an SP3 carbon and not SP2 planar, which would be expected for the carbonyl oxyen atom. Moreover, if the camphor were partially misoriented, then we would expect to see residual $F_o - F_c$ difference density around the carbonyl oxygen atom that we do not. The best model has a 50:50 mix of substrate and 5-*exo*-hydroxycamphor, suggesting that X-ray-driven reduction of the crystals results in substrate hydroxylation. We have never observed this type of behavior with P450cam. The only time we have seen product in P450cam crystals is when the reduced−oxy complex receives

dx.doi.org/10.1021/bi401330c | Biochemistry 2013, 52, 8898−8906

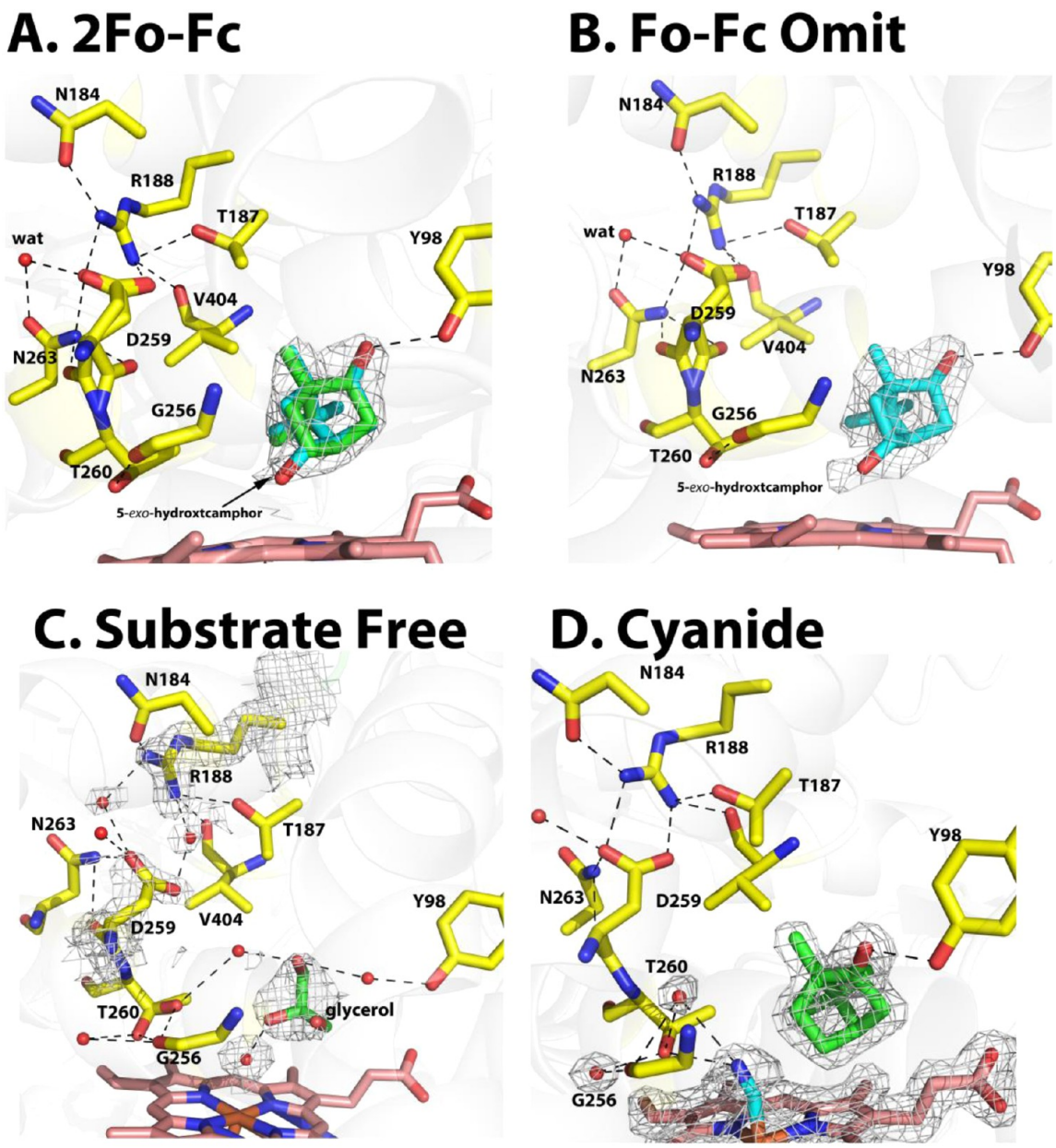

Figure 1. Structures of the wild-type CYP101D1 active site with camphor bound (A and B), in the absence of substrate (C), and in the camphor-bound cyanide complex (D). In panel A, the $2F_o - F_c$ map is contoured at 1.0σ, while in panel B, the omit $F_o - F_c$ map is contoured at 3.0σ. Electron density extending from C5 clearly indicates hydroxycamphor at ~50% occupancy. Hydroxycamphor is colored cyan and camphor green. The substrate-free sructure (C) with glycerol replacing the substrate shows that the ion pair between Asp259 and Arg188 has been disrupted. In the cyanide complex (D), the $2F_o - F_c$ omit electron density is contoured at 1.0σ. Water molecules are represented as red spheres. Electrostatic interactions are represented as black dashed lines.

large doses of X-rays or in crystals of the P450cam−Pdx complex. Thus, CYP101D1 is more susceptible to X-ray-driven O_2 activation and substrate hydroxylation.

Another possibly important difference involves Asp259, which is the essential Asp251 in P450cam. In P450cam, the peptide carbonyl of Asp251 adopts an odd conformation and points perpendicular to the I helix axis rather than parallel as in a normal helix. In CYP101D1, the Asp259 peptide adopts two conformations in molecule A (Figure 1A) of the two molecules in the asymmetric unit, while in molecule B, there is only one conformation. It thus appears that the peptide of Asp259 is more relaxed or flexible in CYP101D1 than the corresponding Asp251 in P450cam. The salt bridge interactions between Asp259 and Arg188 in CYP101D1 appear to be weaker than the corresponding interactions in P450cam (residues in P450cam are Asp251 and Arg186). Unlike Asp251 in P450cam, Asp259 in CYP101D1 must compete with Asn184, Thr187, and Val404, all of which are close enough for electrostatic interactions with Arg188. Most importantly, the Asp251-Lys178 ion pair found in P450cam is missing in CYP101D1 because the Lys178 in P450cam corresponds to Gly180 in CYP101D1. As a result, water takes the place of the missing Lys side chain (Figure 1A). We also estimated the stability of the Asp259-Arg188 ion pair using a computational approach employed earlier for P450cam.[28] As a control, we calculated the stability of the Asp251-Arg186 ion pair in

dx.doi.org/10.1021/bi401330c | *Biochemistry* 2013, 52, 8898−8906

P450cam to be −8.6 kcal/mol, which compares well with the value of −8.44 kcal/mol from the published value.[28] In CYP101D1, the stability of this ion pair is calculated to be −5.9 kcal/mol.

We attempted to obtain the substrate-free structure in hopes of capturing CYP101D1 in the open conformation. However, as in previous studies,[8] substrate-free CYP101D1 crystallized in the closed form, and as in the previous studies, a solvent molecule is in the active site. In our case, this solvent molecule is glycerol, while in the earlier structure, dioxane is bound.[8] Although CYP101D1 remains closed, there clearly is some loosening of the structure in regions important for function. In the substrate-bound state, Asp259 ion pairs with Arg188, which is analogous to the Asp251-Arg186 pair in P450cam. However, in the closed glycerol-bound structure, the Asp259-Arg188 interaction is disrupted and water moves in to form a bridge between Asp259 and Arg188 (Figure 1C). When P450cam adopts the open conformation, the Asp251 ion pairs with neighboring residues are broken and Arg186 adopts a totally different orientation.

CYP101D1−Cyanide Complex. We chose to examine ferric−cyanide complexes because cyanide has been shown to be an excellent mimic of oxy-P450cam.[32] Both O_2 and cyanide binding result in an opening of the I helix, which allows two water molecules to move into the active site and establish an H-bonded network with O_2/CN^- that is thought to be important for O_2 activation. The main question we address here is whether the same changes take place in CYP101D1.

The conformational changes in CYP101D1 upon cyanide binding are very similar to those in P450cam (Figure 1D). The cyanide molecule points toward Thr260, which rotates to form a hydrogen bond with the distal nitrogen atom of CN^-. This further results in a widening of the groove formed by the stretch of residues encompassing Gly256−Thr260. Overall, binding of cyanide to CYP101D1 involves (a) breaking of the Thr260−Gly256 H-bond, (b) movement of the Asp259 peptide to the orientation facing Asn263, and (c) opening of the I helix to accommodate two new water molecules in the active site, each H-bonded to both Thr260 and Gly256 (Figure 1B). Overall, the structure indicates a similar mechanism for proton delivery during oxygen activation in CYP101D1 and P450cam using solvent-assisted proton transfer.

D259N Mutant Crystal Structure. In P450cam, the conserved Asp251 is crucial for shuttling protons from solvent molecules to the iron-bound oxygen molecule.[6,7,33] Structural studies of the oxygen complex of mutant D251N in P450cam showed that the Gly248−Thr252 H-bond did not break, and as a result, the catalytically important water molecules could not enter the active site,[33] resulting in an ∼100-fold decrease in activity.[6,7] In our study, we have introduced the corresponding D259N mutation into CYP101D1 and determined the camphor-bound structure to 2.2 Å resolution (Table 1). The peptide of the Asn259 residue can adopt two alternate orientations as observed for the wild-type enzyme (Figure 2A). In molecule A, we observe the presence of some product in the hydroxycamphor density similar to that of the wild-type enzyme. However, the contribution from hydroxycamphor is much smaller than that of the wild-type enzyme. In D259N mutant molecule A, the occupancy for hydroxycamphor is ∼30%, whereas in molecule B, it was only ∼15−20%. The H-bonding network involving the side chains of Asn259 and Arg188 is altered with the loss of the salt bridge interactions. Arg188 moves away, and new water molecules participate in the

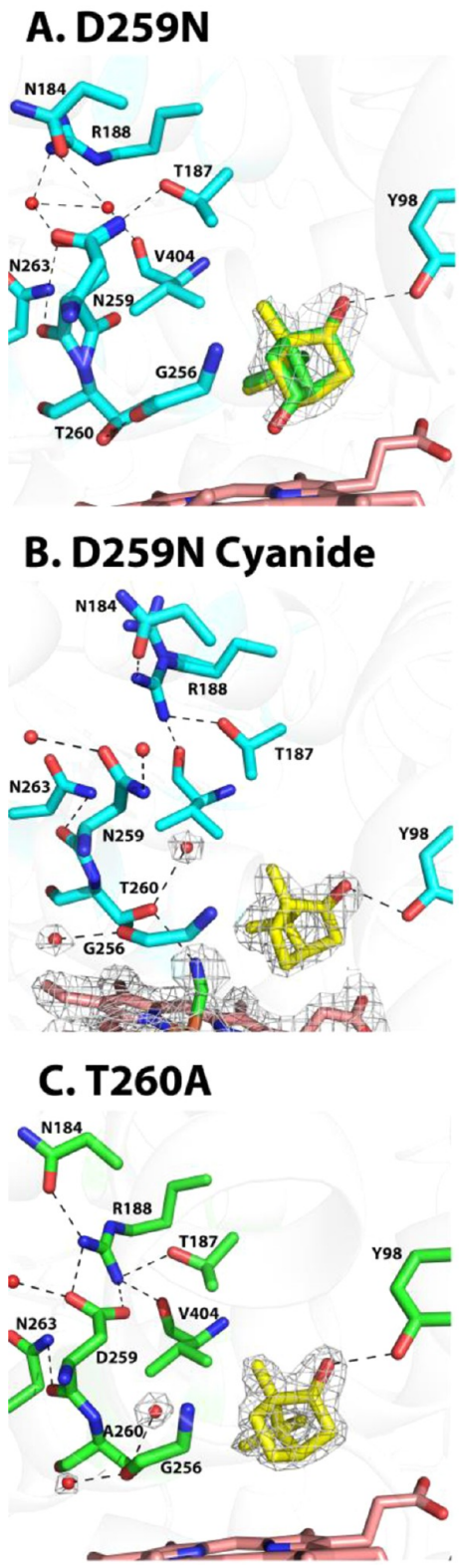

Figure 2. Structures of the CYP101D1 D259N mutant. (A) Camphor-bound structure with the $2F_o - F_c$ electron density map contoured at 1.0σ. The occupancy of hydoxycamphor, ≈30%, is lower than that of the wild type. Hydroxycamphor is colored green and camphor yellow. (B) Cyanide complex with the $2F_o - F_c$ electron density map contoured at 1.0σ. (C) T260A mutant structure with the $2F_o - F_c$ electron density map contoured at 1.0σ. There is no indication of hydroxycamphor.

dx.doi.org/10.1021/bi401330c | *Biochemistry* 2013, 52, 8898−8906

H-bonding network. In the D259N−CN^- complex, the I helix adopts a similar open conformation as in the wild-type CN^- structure that includes two new water molecules (Figure 2B). However, these waters are positioned quite differently. In the wild-type structure, one of the new waters can directly H-bond with CN^-, while in D259N, this water is ∼4.6 Å from the CN^-. The second new water molecule can also only H-bond with Gly256 and not with Thr260. Part of the reason is that Thr260 adopts a different rotamer conformation in D259N that blocks the water from approaching much closer to CN^-. These differences probably result from the I helix moving slightly closer to the CN^- in D259N than in the wild type. In addition, the Asp259-Arg188 ion pair in the wild type more rigidly holds the structure in place, while in D259N, the side chain adopts a new rotamer conformation, leaving Asn259 with no direct protein interactions.

T260A Mutant Structure. Another key residue in P450cam is Thr251. The T251A mutant is highly uncoupled[33−35] and is thought to play an important role in the H-bonding requirements for O_2 activation by possibly helping to stabilize the hydroperoxy intermediate.[33] We introduced the corresponding T260A mutation into CYP101D1 and determined the structure of the camphor-bound complex to 1.8 Å resolution. We attempted to determine the structure of the cyanide complex as well, but the electron density for the cyanide was weak, indicating very low occupancy binding. Therefore, we did not further pursue this structure. Similar to P450cam,[34] in the camphor-bound T260A mutant of CYP101D1, the I helix opens up, thus allowing the two water molecules to enter the active site that are present only in the O_2 or CN^- wild-type structures (Figure 2C). We did not observe any hydroxycamphor density for this mutant in the active site for either molecule in the asymmetric subunit. The H-bonding network involving the side chains of Arg188 and Asp259 is similar to that of the wild-type enzyme.

Steady State Assays. Previously conducted NADH oxidation assays showed that CYP101D1 has high turnover rates, a high coupling efficiency, and a high affinity for camphor (K_d ∼ 9 μM).[8] We performed activity assays with the wild-type and mutant enzymes to test the effects of the D259N and T260A mutations on enzyme activity. Consistent with the earlier studies, wild-type CYP101D1 has high turnover rates comparable to that of P450cam, and the reaction is highly coupled (Table 2). The presence or absence of the N-terminal six-His tag did not have any significant effect on enzyme activity. The T260A mutant retained significant (∼50%) NADH turnover rates compared to that of the wild type, but the reaction is highly uncoupled. On the other hand, the D259N mutation lowers activity to the extent that no significant NADH turnover or product formation could be observed.

Redox Partner Selectivity. Because the recently determined P450cam−Pdx crystal structure[5] strongly implicates Pdx binding as being critical to structural changes involving Asp251 required for proton-coupled electron transfer, we next examined the question of redox partner selectivity in CYP101D1. The supporting proteins for CYP101D1, the Arx ferredoxin and ArR ferredoxin reductase, have structures very similar to those of the P450cam counterparts, Pdx and Pdr, although residues at the docking interfaces are substantially different.[8] We measured the activity of wild-type CYP101D1 using the P450cam redox partners, Pdr and Pdx. As shown in Figure 3, there is a linear increase in activity with an increase in Pdx concentration but does not saturate, although the reaction is significantly coupled (Table 2). This is consistent with relatively robust electron transfer reaction but poor binding of Pdx to CYP101D1 and the possibility that full saturation is not achieved even at the highest concentration of Pdx used, 60 μM. This shows that CYP101D1 is not as selective for its redox partner as P450cam, which further suggests that Arx may not serve a role as a major effector in CYP101D1 as opposed to Pdx, which plays a critical effector role in P450cam. As expected, we failed to observe any significant activity with P450cam using ArR and Arx, the CYP101D1 redox partners.

Table 2. NADH Turnover Rates[a]

P450 type	redox partner	NADH turnover (min^{-1})	coupling efficiency (%)
WT CYP101D1	Arr/Arx	950 ± 42	95
T260A CYP101D1	Arr/Arx	522 ± 20	NA[b]
D259N CYP101D1	Arr/Arx	NA[b]	NA[b]
WT CYP101D1	Pdr/Pdx	40 ± 12	69
WT P450cam	Pdr/Pdx	930 ± 28	95
WT P450cam	Arr/Arx	NA[b]	NA[b]

[a]The reaction mixture contained 0.5 μM Arr, 5 μM Arx, and 0.5 μM P450 in 50 mM Tris (pH 7.4). The values for P450cam were taken from our previous work.[12] The rate of NADH oxidation for CYP101D1 in the presence of either 200 μM or 1 mM D-camphor at room temperature was measured by monitoring the absorbance change at 340 nm using an extinction coefficient of 6.22 mM^{-1} cm^{-1}. No significant differences in rates were observed at the two camphor concentrations. [b]No significant turnover or product formation was observed.

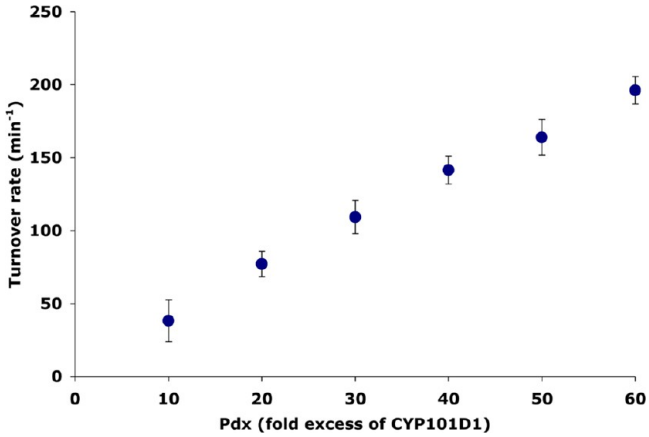

Figure 3. NADH turnover rates for CYP101D1 with the redox partners of P450cam, Pdr and Pdx. The rate increases linearly with increase in Pdx concentration.

DISCUSSION

CYP101D1 was the first P450 to be found that catalyzes exactly the same reaction as P450cam using very similar supporting redox proteins.[14,17] CYP101D1 thus provides an opportunity to probe what structural and functional features must be shared and which can differ yet maintain high catalytic efficiency. One of the more interesting and possibly unusual properties of P450cam is its strict requirement for its own redox partner, Pdx. In addition, camphor shifts the conformational equilibrium of P450cam completely from the open low-spin state to the closed high-spin state.[13] CYP101D1 shares neither of these

dx.doi.org/10.1021/bi401330c | Biochemistry 2013, 52, 8898−8906

properties. Earlier studies[8] as well as our own more recent work show that camphor shifts CYP101D1 to at most 40−45% high-spin, yet CYP101D1 is as active and as tightly coupled as P450cam. In addition, CYP101D1 is not specific for its own ferredoxin electron donor, Arx, because Pdx can substitute for Arx. This suggests that specific protein−protein interactions may not play an effector role in CYP101D1 as important as that in P450cam.

We first address the question of incomplete spin shift in CYP101D1. With P450cam, it now appears that the high-spin substrate-bound state is associated with the closed conformation while the low-spin state is associated with the open state.[13] The closed to open switch in P450cam results in a large structural change involving a significant repositioning of the F and G helices, which effectively exposes the active site to bulk solvent.[13] So far, no structure of an open CYP101D1 has been determined, but an open structure of CYP101D2 has been.[36] The sequences of CYP101D1 and CYP101D2 are 62% identical.[36] Open CYP101D2 has camphor bound but in a nonproductive orientation where the substrate carbonyl oxygen H-bonds with the water ligand coordinated to the heme iron and thus is a substrate-bound low-spin complex. If CYP101D1 also can form a substrate-bound low-spin complex, then reduction of the low-spin form would result in dissociation of the water ligand, which then might allow the camphor to reorient into a productive position. The main difference between P450cam and CYP101D1 then would be that substrate-bound low-spin CYP101D1 can be reduced but not low-spin P450cam and, perhaps, P450cam cannot form a low-spin substrate-bound complex.

To address the question of the effector role of redox partner binding, we first needed to check if the key active site residues important in proton-coupled electron transfer in P450cam are also critical in CYP101D1. As expected, the answer is yes. Both Thr260 and Asp259 are important. The various CYP101D1−CN^- structures also show that CN^- induces very much the same changes in CYP101D1 as it does in P450cam even to the extent that the same "catalytic" waters enter the active site to provide part of the proton delivery machinery. The D259N−CN^- structure is particularly insightful because here the catalytic waters are not properly placed, which also is the effect of this mutation on P450cam. With P450cam, the D251N mutant has much reduced activity but just enough to measure an ∼5-fold increase in the kinetic solvent isotope effect,[37] which strongly argues that Asp251 plays an important role in the delivery of the proton to dioxygen. This view is consistent with our current CYP101D1 results and shows that the proton delivery machinery operates the same in both forms of P450.

It also has been proposed that Asp251 in P450cam is intimately tied to the effector role of Pdx.[5] In the closed conformation, Asp251 is tied up with ion pairs to Lys178 and Arg186, so it is not possible for Asp251 to participate in a proton shuttle network. However, when Pdx binds, these salt bridges are broken, suggesting that one of the main effector roles of Pdx is to free Asp251 to perform its role in proton-coupled electron transfer. Asp259 in CYP101D1 also is tied up with Arg188, but the residue corresponding to Lys178 in P450cam, which also forms an ion pair with D251, is a glycine in CYP101D1. In addition, we found that although substrate-free CYP101D1 with a glycerol molecule in the active site is in the closed conformation, the Asp259-Arg188 ion pair has been broken and replaced by water molecules that bridge these two residues. It thus is easier to free Asp259 in CYP101D1 to serve its role in proton delivery, while P450cam is more firmly tied down in the closed conformation and requires Pdx to provide additional stabilization of the open form, which frees Asp251 from its salt bridges. In sharp contrast, CYP101D1 does not require this extra "help" because the Asp259−Arg188 interaction is more readily disrupted. One final observation indicating that it is easier for CYP101D1 to adopt the active conformation is that the product is observed in electron density maps in CYP101D1 but not in P450cam. If O_2 activation requires proton-coupled electron transfer, then X-ray-induced reduction must be accompanied by the transfer of protons to dioxygen for the hydroxylation of the substrate. The tightly closed conformation in P450cam prevents ready access of bulk solvent protons to the active site, so even upon reduction of the heme iron by X-rays, the product does not form. However, because the active site entry in CYP101D1 is looser, solvent protons can enter more easily and product can be observed.

An equally challenging question to address is the biological advantage or disadvantage of a tightly controlled system like P450cam versus a more promiscuous system like CYP101D1. P450cam is encoded on a plasmid and is part of a tightly regulated operon, so that the P450cam proteins are produced only when needed. When camphor is the only or primary carbon source, it would be critical to efficiently utilize reducing equivalents for only camphor oxidation. Without such selectivity, any low-potential reductant could turn over P450cam, resulting in wasted reducing equivalents not utilized for camphor oxidation in addition to the generation of toxic peroxide and superoxide. Selectivity is achieved by tightly coupling substrate binding to spin state, redox partner binding, and proton-coupled electron transfer. In contrast, CYP101D1 is one of several forms of P450 in *Novosphingobium aromaticivorans*, so camphor oxidation by CYP101D1 is unlikely to be critical for using camphor as a carbon source because one of the other several forms of P450 could serve this function. In addition, *N. aromaticivorans* has only one ferredoxin, Arx, that services several other P450 proteins, which is somewhat reminiscent of mammalian liver P450 proteins in which several promiscuous P450 proteins are supported by a single reductase. In these cases, an additional level of control requiring an effector role for the reductase is not required. It is tempting to speculate that CYP101D1 is representative of a simpler P450 system in which fewer levels of control are required because CYP101D1 is not an essential component in the oxidative assimilation of a specific carbon source and thus is not critical to the survival of the organism. Nature, however, required a higher level of control with P450cam-like systems in which the P450 is an essential component in energy transduction and thus must be more tightly regulated and controlled.

■ ASSOCIATED CONTENT

Accession Codes

Coordinates and structure factors have been deposited in the Protein Data Bank as entries 4C9K, 4C9L, 4C9M, 4C9N, 49CO, and 4C9P.

■ AUTHOR INFORMATION

Corresponding Author

*E-mail: poulos@uci.edu. Phone: (949) 824-7020.

Funding

This work was supported by National Institutes of Health Grant GM33688 and National Institutes of Health/National

Cancer Institute Institutional Training Grant Fellowship T32CA009054.

Notes

The authors declare no competing financial interest.

■ ACKNOWLEDGMENTS

This paper involves research conducted at the Stanford Synchrotron Radiation Laboratory (SSRL), a national user facility operated by Stanford University on behalf of the U.S. Department of Energy, Office of Basic Energy Sciences. The SSRL Structural Molecular Biology Program is supported by the Department of Energy, Office of Biological and Environmental Research, and by the National Institutes of Health, National Center for Research Resources, Biomedical Technology Program, and the National Institute of General Medical Sciences. We thank Dr. Huiying Li and Dr. Irina Sevrioukova for helpful discussions and advice.

■ ABBREVIATIONS

CYP, cytochrome P450; Pdx, putidaredoxin; Pdr, putidaredoxin reductase; ArR, ferredoxin reductase; Arx, [2Fe-2S] ferredoxin; NADH, nicotinamide adenine dinucleotide hydride; GC−MS, gas chromatography−mass spectrometry; WT, wild type.

■ REFERENCES

(1) Tyson, C. A., Lipscomb, J. D., and Gunsalus, I. C. (1972) The role of putidaredoxin and P450 cam in methylene hydroxylation. *J. Biol. Chem. 247*, 5777−5784.

(2) Lipscomb, J. D., Sligar, S. G., Namtvedt, M. J., and Gunsalus, I. C. (1976) Autooxidation and hydroxylation reactions of oxygenated cytochrome P-450cam. *J. Biol. Chem. 251*, 1116−1124.

(3) Nagano, S., Shimada, H., Tarui, A., Hishiki, T., Kimata-Ariga, Y., Egawa, T., Suematsu, M., Park, S.-Y., Adachi, S.-i., Shiro, Y., and Ishimura, Y. (2003) Infrared spectroscopic and mutational studies on putidaredox-induced conformational changes in ferrous CO-P450cam. *Biochemistry 42*, 14507−14514.

(4) Hiruma, Y., Hass, M. A., Kikui, Y., Liu, W. M., Olmez, B., Skinner, S. P., Blok, A., Kloosterman, A., Koteishi, H., Lohr, F., Schwalbe, H., Nojiri, M., and Ubbink, M. (2013) The Structure of the Cytochrome P450cam-Putidaredoxin Complex Determined by Paramagnetic NMR Spectroscopy and Crystallography. *J. Mol. Biol. 425*, 4353−4365.

(5) Tripathi, S., Li, H., and Poulos, T. L. (2013) Structural basis for effector control and redox partner recognition in cytochrome P450. *Science 340*, 1227−1230.

(6) Gerber, N. C., and Sligar, S. G. (1994) A role for Asp-251 in cytochrome P-450cam oxygen activation. *J. Biol. Chem. 269*, 4260−4266.

(7) Gerber, N. S., and Sligar, S. G. (1992) Catalytic mechanism of cytochrome P-450: Evidence for a distal charge relay system. *J. Am. Chem. Soc. 114*, 8742−8743.

(8) Yang, W., Bell, S. G., Wang, H., Zhou, W., Hoskins, N., Dale, A., Bartlam, M., Wong, L. L., and Rao, Z. (2010) Molecular characterization of a class I P450 electron transfer system from *Novosphingobium aromaticivorans* DSM12444. *J. Biol. Chem. 285*, 27372−27384.

(9) Nagano, S., Tosha, T., Ishimori, K., Morishima, I., and Poulos, T. L. (2004) Crystal structure of the cytochrome P450cam mutant that exhibits the same spectral perturbations induced by putidaredoxin binding. *J. Biol. Chem. 279*, 42844−42849.

(10) Lange, R., and Debey, P. (1979) Spin transition of camphor-bound cytochrome P-450. 1. Local paH and electrostatic interactions. *Eur. J. Biochem. 94*, 485−489.

(11) Poulos, T. L., Finzel, B. C., and Howard, A. J. (1987) High-resolution crystal structure of cytochrome P450cam. *J. Mol. Biol. 195*, 687−700.

(12) Batabyal, D., Li, H., and Poulos, T. L. (2013) Synergistic Effects of Mutations in Cytochrome P450cam Designed To Mimic CYP101D1. *Biochemistry 52*, 5396−5402.

(13) Lee, Y. T., Wilson, R. F., Rupniewski, I., and Goodin, D. B. (2010) P450cam visits an open conformation in the absence of substrate. *Biochemistry 49*, 3412−3419.

(14) Bell, S. G., and Wong, L.-L. (2007) P450 enzymes from the bacterium *Novosphingobium aromaticivorans*. *Biochem. Biophys. Res. Commun. 360*, 666−672.

(15) Sevrioukova, I. F., and Poulos, T. L. (2002) Putidaredoxin reductase, a new function for an old protein. *J. Biol. Chem. 277*, 25831−25839.

(16) Sevrioukova, I., Gracia, C., Li, H., Bhaskar, B., and Poulos, T. L. (2003) Crystal structure of putidaredoxin, the [2Fe-2S] component of the P450cam monooxygenase system from *Pseudomonas putida*. *J. Mol. Biol. 333*, 377−392.

(17) Bell, S. G., Dale, A., Rees, N. H., and Wong, L.-L. (2010) A cytochrome P450 class I electron transfer system from *Novosphingobium aromaticivorans*. *Appl. Microbiol. Biotechnol. 86*, 163−175.

(18) Kuznetsov, V. Y., Blair, E., Farmer, P. J., Poulos, T. L., Pifferitti, A., and Sevrioukova, I. F. (2005) The putidaredoxin reductase-putidaredoxin electron transfer complex: Theoretical and experimental studies. *J. Biol. Chem. 280*, 16135−16142.

(19) Gunsalus, I. C., and Wagner, G. C. (1978) Bacterial P-450cam methylene monooxygenase components: Cytochrome m, putidaredoxin, and putidaredoxin reductase. *Methods Enzymol. 52*, 166−188.

(20) Sevrioukova, I., Hazzard, J. T., Tollin, G., and Poulos, T. L. (2001) Laser flash induced electron transfer in P450cam monooxygenase: Putidaredoxin reductase-putidaredoxin interaction. *Biochemistry 40*, 10592−10600.

(21) Churbanova, I. Y., Poulos, T. L., and Sevrioukova, I. F. (2010) Production and characterization of a functional putidaredoxin reductase-putidaredoxin covalent complex. *Biochemistry 49*, 58−67.

(22) Battye, T. G., Kontogiannis, L., Johnson, O., Powell, H. R., and Leslie, A. G. (2011) iMOSFLM: A new graphical interface for diffraction-image processing with MOSFLM. *Acta Crystallogr. D67*, 271−281.

(23) Kabsch, W. (2010) Xds. *Acta Crystallogr. D66*, 125−132.

(24) Otwinowski, Z., and Minor, W. (1997) in *Macromolecular Crystallography, Part A*, Vol. *276*, pp 307−326, Elsevier, Amsterdam.

(25) McCoy, A. J., Grosse-Kunstleve, R. W., Adams, P. D., Winn, M. D., Storoni, L. C., and Read, R. J. (2007) Phaser crystallographic software. *J. Appl. Crystallogr. 40*, 658−674.

(26) Winn, M. D., Ballard, C. C., Cowtan, K. D., Dodson, E. J., Emsley, P., Evans, P. R., Keegan, R. M., Krissinel, E. B., Leslie, A. G. W., McCoy, A., McNicholas, S. J., Murshudov, G. N., Pannu, N. S., Potterton, E. A., Powell, H. R., Read, R. J., Vagin, A., and Wilson, K. S. (2011) Overview of the CCP4 suite and current developments. *Acta Crystallogr. D67*, 235−242.

(27) Adams, P. D., Afonine, P. V., Bunkoczi, G., Chen, V. B., Davis, I. W., Echols, N., Headd, J. J., Hung, L. W., Kapral, G. J., Grosse-Kunstleve, R. W., McCoy, A. J., Moriarty, N. W., Oeffner, R., Read, R. J., Richardson, D. C., Richardson, J. S., Terwilliger, T. C., and Zwart, P. H. (2010) PHENIX: A comprehensive Python-based system for macromolecular structure solution. *Acta Crystallogr. D66*, 213−221.

(28) Lounnas, V., and Wade, R. C. (1997) Exceptionally stable salt bridges in cytochrome P450cam have functional roles. *Biochemistry 36*, 5402−5417.

(29) Hendsch, Z. S., and Tidor, B. (1994) Do salt bridges stabilize proteins? A continuum electrostatic analysis. *Protein Sci. 3*, 211−226.

(30) Gilson, M. K., and Honig, B. H. (1987) Calculation of electrostatic potentials in an enzyme active site. *Nature 330*, 84−86.

(31) Wang, J., Wolf, R. M., Caldwell, J. W., Kollman, P. A., and Case, D. (2004) Development and testing of a general Amber force field. *J. Comput. Chem. 25*, 1157−1174.

(32) Fedorov, R., Ghosh, D. K., and Schlichting, I. (2003) Crystal structures of cyanide complexes of P450cam and the oxygenase domain of inducible nitric oxide synthase: Structural models of the short-lived oxygen complexes. *Arch. Biochem. Biophys. 409*, 25−31.

(33) Nagano, S., and Poulos, T. L. (2005) Crystallographic study on the dioxygen complex of wild-type and mutant cytochrome P450cam: Implications for the dioxygen activation mechanism. *J. Biol. Chem. 280*, 31659−31663.
(34) Raag, R., Martinis, S. A., Sligar, S. G., and Poulos, T. L. (1991) Crystal structure of the cytochrome P-450CAM active site mutant Thr252Ala. *Biochemistry 30*, 11420−11429.
(35) Kimata, Y., Shimada, H., Hirose, T., and Ishimura, Y. (1995) Role of Thr-252 in cytochrome P450cam: A study with unnatural amino acid mutagenesis. *Biochem. Biophys. Res. Commun. 208*, 96−102.
(36) Yang, W., Bell, S. G., Wang, H., Zhou, W., Bartlam, M., Wong, L. L., and Rao, Z. (2011) The structure of CYP101D2 unveils a potential path for substrate entry into the active site. *Biochem. J. 433*, 85−93.
(37) Vidakovic, M., Sligar, S. G., Li, H., and Poulos, T. L. (1998) Understanding the role of the essential Asp251 in cytochrome p450cam using site-directed mutagenesis, crystallography, and kinetic solvent isotope effect. *Biochemistry 37*, 9211−9219.
(38) Karplus, P. A., and Diederichs, K. (2012) Linking crystallographic model and data quality. *Science 336*, 1030−1033.